AIAA JOURNAL
Vol. 32, No. 6, June 1994

Low-Dimensional Description of the Dynamics in Separated Flow past Thick Airfoils

Anil E. Deane*
NASA Goddard Space Flight Center, Greenbelt, Maryland 20771
and
Catherine Mavriplis†
George Washington University, Washington, D.C. 20052

Results are presented for the numerical simulation of unsteady viscous incompressible flow past thick airfoils. Specifically, flow past a NACA 4424 at an angle of attack of 2.5 deg and Reynolds numbers in the range of 1700–4000 has been simulated using the spectral element method. At these conditions the flow is separated and an unsteady wake is formed. Application of the method of empirical eigenfunctions reveals the structure of the most energetic components of the flow. These are found to occur in pairs that, through phase exchange, are responsible for the vortex shedding. A set of ordinary differential equations is obtained for the amplitudes of these eigenfunctions by a Galerkin projection of the Navier-Stokes equations. The solutions of the model system are compared with the full simulation. The work is of relevance to the transition process and observed routes to chaos in airfoil wakes.

Introduction

THE unsteady flow past an airfoil is an example of a complex flow of great engineering relevance that involves many spatial and temporal scales. At Reynolds numbers of practical significance the flow is so complicated that numerical simulations of the flow represent major research efforts. Apart from coupling inviscid/viscous interactions through the boundary layer, turbulence modeling is employed to account for the small-scale behavior. Direct numerical simulations on the other hand are limited to modest Reynolds numbers which are usually too low for engineering purposes. Nevertheless, these simulations are useful in investigating the nonlinear interaction in transitional and weakly turbulent flows, since, other than the usual numerical approximations, no additional assumptions are necessary. The spectral element method,[1] which combines the advantages of finite element methods in allowing complex geometries and the fast convergence properties of spectral methods, has become a practical tool for this investigation.[2] Recently, the method of empirical eigenfunctions[3,4] has been utilized as a method of analyzing complicated turbulent flow data. When applied using an ensemble of flow realizations the method yields a set of orthogonal functions that are best able to account for the energy of the system as represented by the ensemble. Much can be learned about the flow by consideration of the structure and interaction of these functions or modes. In this paper, and in other work,[5] we combine the methodologies of direct spectral element simulations and empirical eigenfunctions.

In applying the method of empirical eigenfunctions we wish to understand the wake system of flow past an airfoil both in terms of the nature of the large-scale structures and that of the disturbances that induce transition. As a start we restrict our attention to a relatively thick airfoil at modest Reynolds numbers. With the chosen geometry and parameter values the flow is separated over the rear of the airfoil and appears aperiodic. We apply the method to data obtained from numerical simulations. The derived eigenfunctions reveal the nature of the large-scale structures observable in the flow. By using the set of the derived orthogonal functions as a basis for a Galerkin approximation we obtain sets of ordinary differential equations for the amplitudes of these modes. By retaining only a small number of the modes in the Galerkin approximation a low-dimensional description is assured. The resulting system of equations is integrated and comparisons are made with the full simulation.

Recently, transition from laminar to turbulent states has been studied in terms of ideas from low-order dynamical systems in open flow systems. Gharib and Williams-Stuber[6] and Williams-Stuber and Gharib[7] used strip-heater forcing to study wave amplification, interaction, and cancellation and eventual routes of transition to chaos in the wake behind a slender airfoil. They used a slender airfoil with forcing to concentrate on the convective instability in the far wake (away from the trailing edge.) Similar studies have been made by Sreenivasan[8] on instabilities induced by forcing in the wake of a circular cylinder. In the present case we use a thick airfoil at an angle of attack to capture both the far-wake region instability and the near-field region of absolute instability. Our work complements the forced wake studies.

We find a close correspondence between the results reported here and those for a circular cylinder.[5] Many of the features observed here appear to be common to wake flows in general. The method of empirical eigenfunctions provides a natural way to quantify the similarities.

The central goal of this work is to understand the transition process in general and in particular on aircraft wings. The method of empirical eigenfunctions is a tool which can significantly reduce computational effort for flow simulations. Once an eigenfunction decomposition has been made, the ordinary differential equation system is relatively trivial to solve and can therefore cover a wide parameter range. Ultimately this method could be used in design or control applications to prevent or delay separation and transition. This paper, however, only lays the groundwork for the development of such a design tool. It is essential that a one-to-one comparison of the direct simulation and the empirical eigenfunction model be made so that it may be understood and proven that this method can be an effective tool.

Direct Numerical Simulation of Separated Flow

The separated flow past a thick airfoil is computed by direct simulation of the unsteady incompressible Navier-Stokes equations using a spectral element method. The spectral element solution provides highly accurate data for the application of the method of empirical eigenfunctions which is essential for the

Received March 1, 1993; revision received Oct. 1, 1993; accepted for publication Oct. 4, 1993.

*Research Scientist, Universities Space Research Association, MC 934.
†Assistant Professor, Civil, Mechanical, and Environmental Engineering. Member AIAA.

method's success and that of the subsequent low-dimensional description.

The methodology of the spectral element method has been the subject of many papers, e.g., Refs. 1, 2, and 9, and therefore is not described here. The basic premise of this method is a domain decomposition into macro-elements upon each of which all dependent and independent variables are described as tensor products of high-order Legendre-Lagrangian polynomial interpolants. Taking advantage of the orthogonality of the set of polynomials, all terms can be efficiently calculated by tensor product factorization. The final equations are obtained by rewriting the incompressible Navier-Stokes equations in Galerkin variational form and discretizing. The discrete system is solved efficiently by preconditioned conjugate gradient iteration. The time stepping is a high-order fractional time stepping technique.[2] Fast (exponential) convergence and good resolution properties of the method favor it over low-order discretization techniques.

We are interested in separated flows past thick airfoils in order that we may study fairly complex wake dynamics at Reynolds numbers sufficiently low that direct simulation is viable. We chose a NACA 4424 airfoil following some experiments of Krause et al.[10] The specific conditions we simulated were at an angle of attack of $\alpha = 2.5$ deg in a range of Reynolds numbers from 1700 to 4000 where Reynolds number is defined as $Re = U_\infty c/\nu$, U_∞ being the freestream velocity (= 1), c the chord, and, ν kinematic viscosity.

Figure 1 shows the spectral element grid representing the domain decomposition into macro-elements upon each of which there are $(N+1)\times(N+1)$ collocation points (not shown here). For the solutions presented here $N = 4$. The grid contains a total of 408 elements over a domain of two chord lengths ahead of the airfoil, eight behind and two above and below. The airfoil surface is described by 21 elements which use Nth-order polynomials to conform to the definition of the NACA 4424 profile. The grid was obtained by an interactive block decomposition method[11] adapted to spectral element methods and using a posteriori error estimators[12] to indicate where greater resolution was needed. The boundary conditions are specified freestream velocity at the inlet

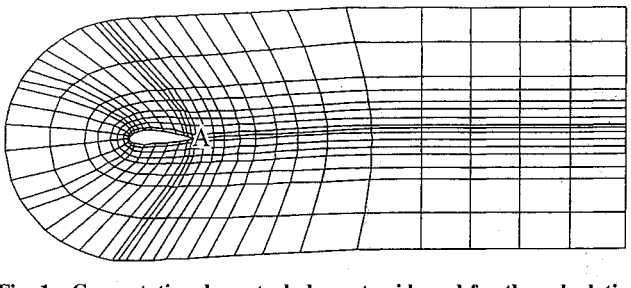

Fig. 1 Computational spectral element grid used for the calculation of flow past NACA 4424 airfoil for all Reynolds numbers investigated.

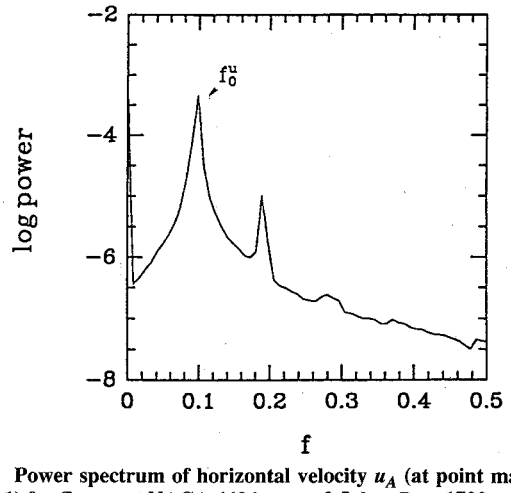

Fig. 2 Power spectrum of horizontal velocity u_A (at point marked A in Fig. 1) for flow past NACA 4424 at $\alpha = 2.5$ deg, $Re = 1700$.

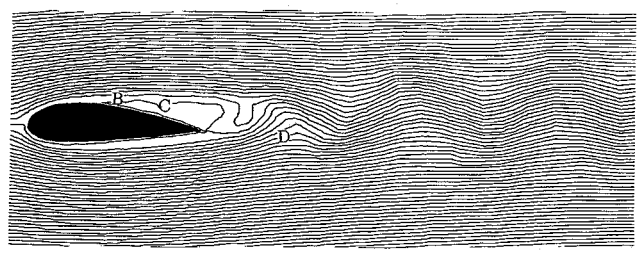

Fig. 3 Streamlines for flow past NACA 4424 at α =2.5 deg, Re = 3000.

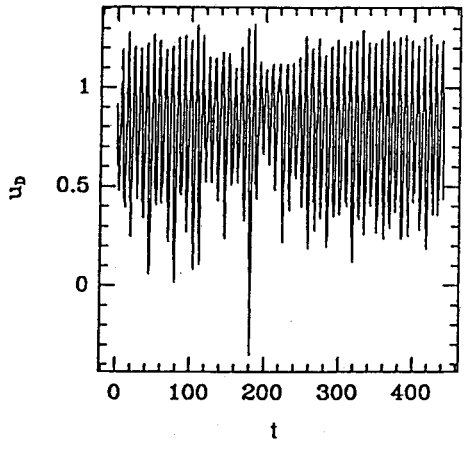

Fig. 4 Re = 3000 time history of horizontal velocity, u_D (at point marked D in Fig. 3).

and on top and bottom boundaries and outflow at the back. In addition we implement a modified Neumann/viscous sponge boundary condition at the exit to stabilize the through flow of large vortices. This procedure is detailed in Karniadakis et al.[13]: essentially, the viscosity is increased across the last two columns of elements preceding the outflow boundary. In the computation a particular run was started from previously fully developed flow at Reynolds numbers in the same range and data was retained only after a period of adjustment.

The 408 × 5 × 5 grid was used for several reasons. First, the same elemental grid was used with $N = 6$ yielding a 408 × 7 × 7 solution. Results were compared for these two grids and appeared qualitatively similar. Because of the limited storage and CPU time available and the large amounts of data required to do the eigenfunction decomposition, the smaller grid (408 × 5 × 5) was used as it uses half the time and half the storage. A posteriori error estimators[12] were used to establish the quality of the results. The overall $\mathcal{L}^2$ error norm for u velocity in the x direction was 0.022. Recall that the freestream velocity is 1. Error estimators were calculated in each element at a specific instant in time (after two cycles) and compared to maximum velocities on the element to yield percent $\mathcal{L}^2$ error norms. Out of 408 elements, there were only two elements where the error was 10% or above: these were 10% and 12%, 75 elements had errors between 1% and 10%, 207 between 0.1% and 1%, 119 between 0.01% and 0.1% and, finally, five between 0.001% and 0.01%. Typically, we can expect an increase in the polynomial order from $N = 4$ to $N = 6$ to gain one order of magnitude in accuracy.

Within the chosen range of Reynolds number there appears to be a transition from a periodic to a quasiperiodic or aperiodic wake. At $Re = 1700$, for instance, the flow is periodic (Fig. 2) with a shedding frequency $f_0 = 0.099$. All quoted frequencies are actual dimensional frequencies. For reference, the nondimensional frequency given by the Strouhal number, St, may be related in the following way: $f = U_\infty St/c$ where $c = 10.091$. A typical instantaneous velocity field of the flow, represented by streamlines, is shown in Fig. 3 for $Re = 3000$. Note the large separation zone on the suction surface

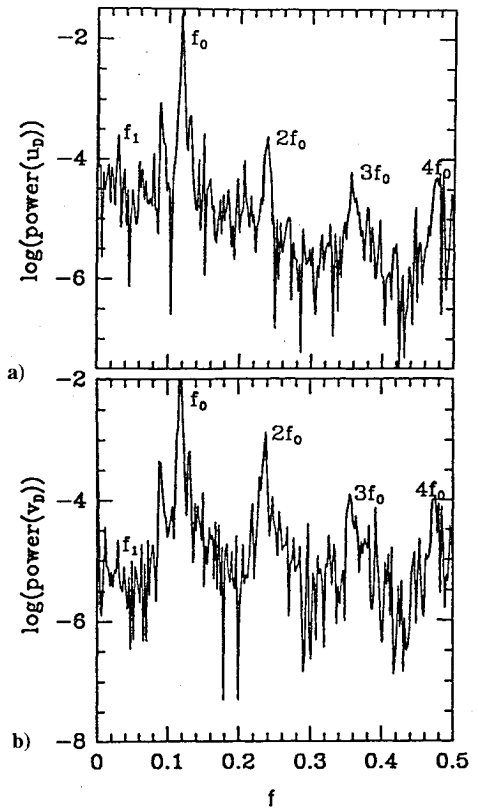

Fig. 5 ***Re*** **= 3000 power spectra of horizontal, a)** u_D**, and vertical, b)** v_D**, velocities.**

and the seemingly disordered formation into a wake at the trailing edge. The time trace of the horizontal velocity component at a point in the near wake is shown in Fig. 4 for $Re = 3000$. Time traces obtained in other regions of the wake show similar features. Figure 5 shows the corresponding power spectra for the flow at $Re = 3000$. The power spectra contain a large number of frequencies with a dominant peak at the shedding frequency $f_0 = 0.118$ with its harmonics at $2f_0$, $3f_0$, and $4f_0$. Another, lower frequency, peak at $f_1 = 0.028$ is also indicated. We return to this figure and comment on these features later. Spectra of points near the separation line (Fig. 6) display similar characteristics (shedding and modulating frequencies) to those obtained elsewhere in the flow. Thus the flow shows global instability characteristics and disturbances are not likely to be simply advected downstream. In summary, in the range of Reynolds number considered here, the flow is seen to be both spatially and temporally complicated.

Method of Empirical Eigenfunctions

We briefly describe the method of empirical eigenfunctions here. More complete treatments are given in Lumley[3] and Sirovich.[4] The objective of the procedure is to obtain basis functions from a set of flow realizations, any one of which is then obtainable from the set of these functions by linear combination. The eigenfunctions of the velocity covariance matrix are found to possess the property that they constitute an orthogonal set which is the smallest set required to capture a given amount of the energy of the system. The data obtained through direct numerical simulation constitutes an ensemble of velocity and pressure fields at several (M) instants in time. If we separate the data into mean $\boldsymbol{U}$ and time-varying parts $\boldsymbol{u}$, e.g.,

$$\boldsymbol{v}(\boldsymbol{x}, t) = \boldsymbol{U}(\boldsymbol{x}) + \boldsymbol{u}(\boldsymbol{x}, t) \tag{1}$$

then the velocity covariance matrix is obtained as,

$$\boldsymbol{R}_{i,j} = \frac{1}{M} \sum_{m=1}^{M} \boldsymbol{u}(\boldsymbol{x}_i, t_m)\boldsymbol{u}(\boldsymbol{x}_j, t_m) \qquad i, j = 1, 2, \ldots, N \tag{2}$$

Here $\boldsymbol{x}_i$ refers to each collocation point and N is their total number. The times t_m are the discrete times at which the fields are obtained.

The eigenvectors, ϕ_j, of this matrix have the property that they form a complete orthonormal set (when properly normalized) and have eigenvalues λ_j that quantify the probability of their occurrence in the flow so that

$$\lambda_m = \langle \{\boldsymbol{u}, \phi_m\}^2 \rangle \tag{3}$$

where braces denote the inner product and angle brackets denote an ensemble average. The sum of these eigenvalues gives the total energy E of the system,

$$E = \sum_{m=1}^{M} \lambda_m \tag{4}$$

The eigenvectors are by construction incompressible,

$$\nabla \cdot \phi_m = 0 \tag{5}$$

and satisfy the boundary conditions. The velocity at any instant can therefore be expanded in terms of these eigenvectors as,

$$\boldsymbol{u}(\boldsymbol{x}, t) = \sum_{m=1}^{M} a_m(t)\phi_m(\boldsymbol{x}) \tag{6}$$

so that

$$a_i(t) = \{\boldsymbol{u}(\boldsymbol{x}, t), \phi_i(\boldsymbol{x})\} \tag{7}$$

Equation (6) forms the basis of a Galerkin expansion.

Results

An ensemble of 40 data sets over a time interval corresponding to four shedding cycles at $Re = 3000$ was collected at the end of the interval shown in Fig. 4. An ensemble for $Re = 4000$ was similarly

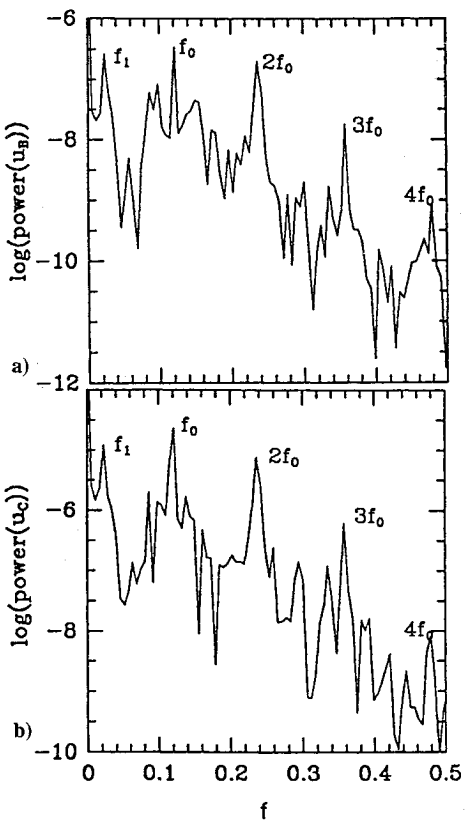

Fig. 6 ***Re*** **= 3000 power spectra of the horizontal velocities, a)** u_B **and b)** u_C**; note that peaks do not appear as sharp as in Fig. 5 since spectra are based on only 40% of the time interval.**

Table 1 Eigenvalues of the modes and their respective contributions to the total energy for the indicated Reynolds numbers; λ is the normalized eigenvalue of the mode representing its fractional contribution to the total energy; the % energy shown is the cumulative energy

	$Re = 3000$		$Re = 4000$	
Index	λ	% energy	λ	% energy
1	0.37823	37.823	0.33612	33.612
2	0.34249	72.072	0.31171	64.783
3	0.04228	76.301	0.04548	69.331
4	0.04073	80.374	0.04003	73.334
5	0.03878	84.252	0.03163	76.497
6	0.03491	87.743	0.02978	79.475
7	0.01741	89.484	0.02306	81.781
8	0.01604	91.088	0.02059	83.839
9	0.01165	92.253	0.01729	85.569
10	0.01133	93.386	0.01671	87.239
11	0.01096	94.481	0.01436	88.675
12	0.01010	95.491	0.01342	90.018
13	0.00851	96.342	0.01248	91.266
14	0.00712	97.054	0.01187	92.453
15	0.00687	97.741	0.00997	93.449
16	0.00560	98.302	0.00965	94.415
17	0.00531	98.833	0.00874	95.289
18	0.00291	99.124	0.00701	95.989
19	0.00134	99.258	0.00666	96.655
20	0.00098	99.356	0.00632	97.287

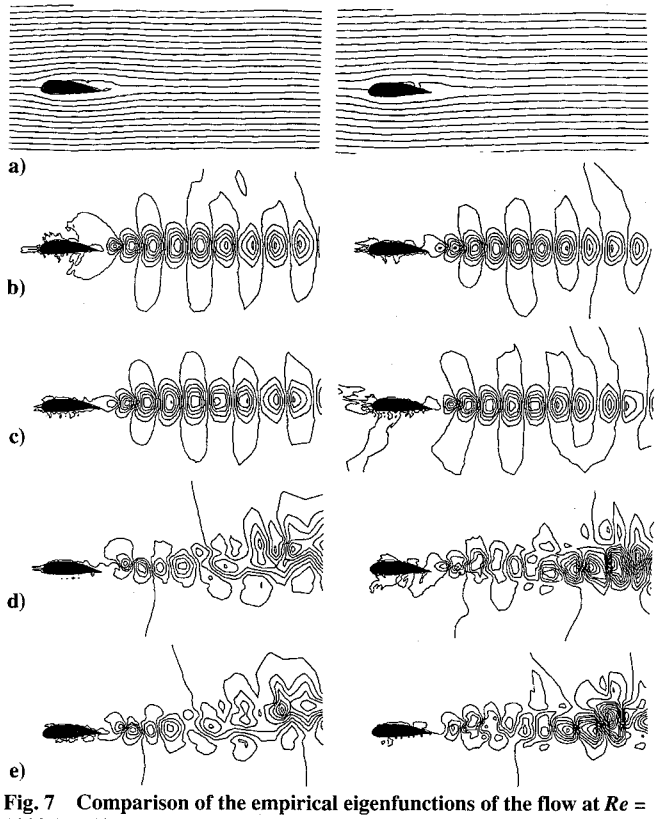

Fig. 7 Comparison of the empirical eigenfunctions of the flow at Re = 3000 (set A) and Re = 4000 (set B); in a) the mean flow and in b)–e) the four most energetic eigenfunctions.

obtained. The resulting eigenfunctions of the covariance matrix have the eigenvalues listed in Table 1. From Eq. (4) the eigenvalues represent an eigenfunction's individual contribution to the total energy. Hence the eigenvalues in Table 1 are ordered from the most energetic to the least energetically significant modes. The eigenvalues appear to occur in pairs of similar values. As found for the cylinder flow[5] vortex shedding can be understood as the exchange of phase between members of the pairs. As we shall see later the modes with lesser energy involve smaller spatial scales. Comparing the two Reynolds numbers we see that the energy is spread over a greater number of modes as Reynolds number increases. For example the first 10 modes at Re = 3000 comprise 93.4% of the total energy, while at Re = 4000 they comprise 87.2% of the total energy.

In Fig. 7 we show the corresponding spatial structure of the eigenfunctions for these two Reynolds numbers. The mean flow is also displayed. Recall that the perturbation field is represented by a linear combination of the eigenfunctions. The most energetic modes ϕ_1 (Fig. 7b) and ϕ_2 (Fig. 7c) comprise the large-scale features of the flow while modes with smaller eigenvalues contain smaller-scale features. Thus the motion can be thought of as a pattern of large vortices with a distribution of smaller and smaller vortices that serve to modify the summation to finally make up an individual realization. The spatial structures of the modes within a pair are seen to be of similar scale but are roughly $\pi/2$ out of phase in the streamwise direction. The change in spatial wavenumber as the Reynolds number is changed is also clearly manifested in the structure of ϕ_1 and ϕ_2. For example comparing ϕ_1^{3000} and ϕ_2^{4000}, there are approximately nine velocity maxima within x = 47 (3.7 chord lengths downstream of the trailing edge) for Re = 3000 as

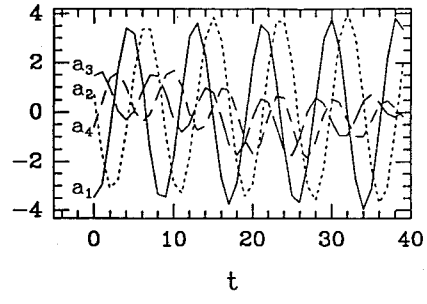

Fig. 8 Projection of the eigenfunction amplitudes (7) for Re = 3000.

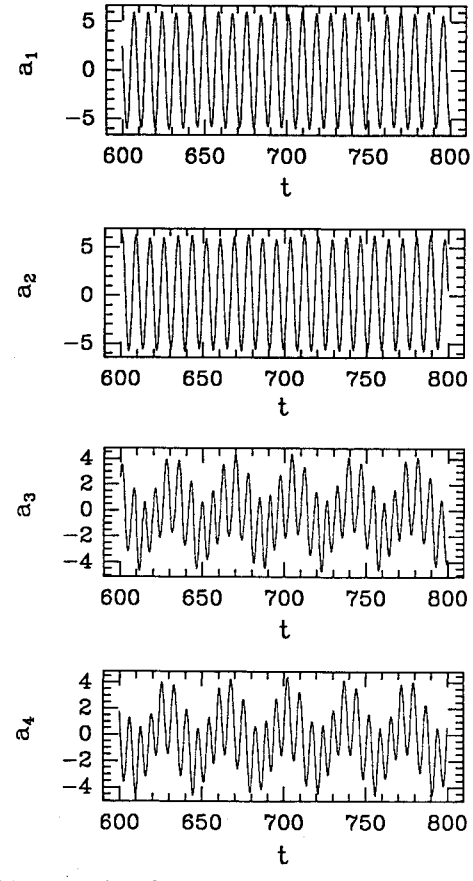

Fig. 9 Time evolution of the eigenfunction amplitudes as obtained by integration of the model system for Re = 3000.

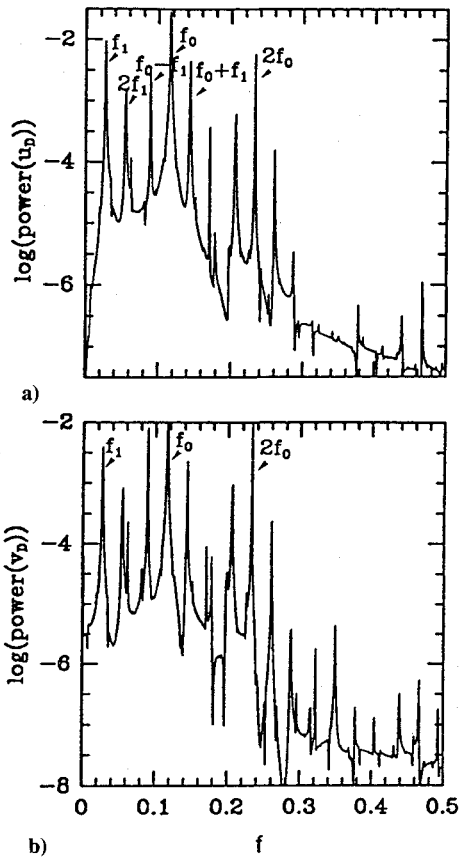

Fig. 10 Power spectra of velocities a) u_D and b) v_D reconstructed from the model for Re = 3000.

compared to ten such maxima for Re = 4000 even though the first maximum is approximately at the same location.

Once the spatial structure has been determined, the amplitude of the eigenfunctions as realized in the ensemble is obtained by the projection (7). This is shown for the most energetic four modes in Fig. 8. The oscillatory nature of the flow is represented by oscillations in the amplitudes of the modes which have fixed spatial structure. Further, the modes are seen to be approximately $\pi/2$ out of phase in time with each other within a pair in the streamwise direction. This coupled with the discrepancy in phase in space (streamwise direction) leads to the traveling character of the vortex street. The higher modes oscillate with a correspondingly higher frequency and maintain the traveling character in a similar manner. Since the flow is oscillatory but aperiodic, the maxima of the amplitudes vary somewhat in time.

These features are entirely analogous to that found in the flow past a cylinder.[5] The pairing and phasing properties are therefore likely to be fundamental to wake flows. The differences in detail are two-fold. Firstly, there is a lack of geometrical symmetry in the case of the airfoil flow. Even a symmetrical airfoil at an angle of attack lacks this symmetry which is reflected here in the modes. The modes ϕ_1 and ϕ_2 appear approximately symmetrical along the midplane but the higher modes, e.g., ϕ_3 and ϕ_4, do not. The second feature is the presence of lift. On a cylinder shedding is symmetrical so that the cylinder feels a lift force that oscillates periodically and the net (time-averaged) lift is zero. On the airfoil due to the camber and angle of attack the net lift is nonzero. The net lift is due to the asymmetric mean field (Fig. 7a). This is not a feature addressed by the decomposition. However the perturbation field contributes the fluctuations in the lift and this is currently being investigated. Similar considerations for the drag force are also underway.

Since the eigenfunctions form an orthogonal basis set we can project the Navier-Stokes equations onto this basis set to obtain differential equations for the evolution of their amplitudes.[5] We retain the M = 12 most energetic modes in the projection which represent approximately 95% of the energy (Table 1) for Re = 3000. The resulting equations written symbolically are

$$\frac{da_i}{dt} = c_i^1 + c_{i,j}^2 a_j + c_{i,j,k}^3 a_j a_k + \frac{1}{Re}(c_i^4 + c_{i,j}^5 a_j) \tag{8}$$

The coefficients c^q arise from the various inner products of the modes with the Navier-Stokes equations. We integrate this set of M = 12 ordinary differential equations numerically to obtain solutions for the amplitudes a_i. In Fig. 9 we show the time evolution of the amplitudes a_i, i = 1, 4. This can be compared with the corresponding projections obtained from the ensemble data (Fig. 8). The mode amplitudes a_1 and a_2 obtained from their dynamical evolution are larger than what they are through projection in the ensemble. The higher modes a_3 and a_4 obtained through evolution show characteristic oscillations extending over considerably larger amplitudes than do the projections.

The computational requirements of the full simulation are evidently very large. To compare with the ordinary differential equations model some typical CPU times are given here. Times are quoted for a Convex C220 using vectorized code. The initial startup of the flow was calculated for a very long time (as shown in Fig. 4) to try to isolate any influence of the initial conditions. In this case, the startup flow was calculated for approximately 10 h. Then the calculation of the four shedding cycles required 1.2 h. The eigenfunction calculation required 10 min, while the projection to obtain the ordinary differential equations required 3 h. Finally, solution over many hundreds of cycles of the 12 ordinary differential equation system required 10 min. Once the decomposition has been done, the ordinary differential equation model is calculated quickly. This is the central advantage of the method. The choice of M is currently based on experience, since this is the first time the method of empirical eigenfunctions has been applied to a flow of Reynolds number in the $\mathcal{O}(10^3)$ range. For M = 2 (or 72% of the energy) and M = 6 (or 87% of the energy) the equations are unstable. In comparison, for the cylinder,[5] M = 6 modes represented 99.9% of the energy and were sufficient to obtain asymptotic stability and the initial (Hopf) bifurcation. For the present case, the energy is spread over a larger number of modes because of the weakly turbulent flow in this, significantly higher, Reynolds number range. Hence a larger number of modes M must be retained.

Figure 10 shows power spectra from the flow formed by a reconstruction, Eq. (6), with M = 12 at a point $\boldsymbol{x} = \boldsymbol{x_D}$ in the wake. Both velocity components are shown. (Note that a reconstructed spectrum of the velocity at a point is similar to that of an individual a_i in harmonic content. The linear summation does not destroy nor create frequency peaks). The motion represented in the model appears to be quasiperiodic, with only discrete frequencies involved. The frequency peak f_0 = 0.115, prominent in the spectra, is found to be very close (2.5% error) to that in the full simulation (Fig. 5). A second frequency marked f_1 = 0.027 is also indicated in the power spectra of the model system and is also very close (3.7% error) to the peak f_1 in the full simulation. All other frequencies in the model spectra are of the form $nf_0 \pm mf_1$, some more prominent than others. Other general features of the model spectra, such as ratio of peaks and decay with large frequency, are unlike that of the full system. It is difficult to determine from the power spectrum of the full simulation if it is a discrete spectrum with possibly superposed continuous noise.

Conclusions

The viscous flow past a thick airfoil has been simulated in the transitional regime. The simulations have provided data for decomposition into empirical eigenfunctions. The structure of these modes is such that the vortex shedding past the airfoil can be understood in terms of the interaction of pairs of modes ordered in their contribution to the kinetic energy of the system. Thus the motion obtained by the model system is at least grossly similar to that of the full system.

A low-dimensional description of the flow has been obtained for this flow in terms of these modes. A model which retains 95% of

the energy of the motion is found, while not reproducing the detailed flow properties, to capture certain essential dynamical features, namely the shedding frequency and its low frequency modulation. Thus gross features of the weakly turbulent flow past a separated airfoil can be captured by a small set of ordinary differential equations. This completes a preliminary investigation of the usefulness of the technique.

Important issues remain which are under investigation. Firstly, the ensemble size is important. Our modes are based on 40 realizations of the flow. These cover four cycles of the airfoil's oscillation history. As such, portions of the phase space domain not visited during this ensemble interval, but which are visited outside the interval, are inaccessible to the model. Secondly, the number of retained modes is important. We have concentrated here on limiting the truncation to 95% of the energy. The absence of higher modes changes the energy spectrum distributed over the modes. Lower modes (e.g., ϕ_1 and ϕ_2) have larger amplitudes than what they would if the complete hierarchy were retained. It has been our experience that simply retaining the complete set is not useful for the dynamical evolution. This is because the highest few modes are so strongly influenced by the ensemble size (i.e., converge slowly with increasing ensemble size) that their dynamical evolution is a large source of error. Thus a larger ensemble is presently being constructed.

Lastly, the simulations themselves reveal important features worthy of investigation. In particular, questions relating to the route followed into turbulence in the unforced wake. From the available simulation data it is possible that a quasiperiodic state has appeared at $Re = 3000$. What are the sources of the incommensurate low-frequency modulations? And is this a quasiperiodic route to chaos (a low-dimensional phenomenon)? And finally, do the model systems undergo similar transitions? These and other issues will be addressed in future work.

While important questions remain concerning the transition process and the parameters of the eigenfunction expansion, it is clear that the basic utility of the method of empirical eigenfunctions has been demonstrated for complex geometries of engineering interest. While the Reynolds number range is low, it is the relevant range for transition studies. Direct simulations of this complexity are just starting to appear in the literature, whereas they have been mostly restricted to relatively simple geometries such as the flat plate, for example, in transition studies. In this paper, the procedure of the method has been verified for a higher range of Reynolds number and a geometrically, spatially, and temporally more complex case than has been attempted before.[5] Ultimately, once the behavior of the method is fully understood and proven (in terms of accuracy), it will be used to cover a wide range of parameter space with relatively trivial computational cost. For example, with one eigenfunction decomposition at a particular point in parameter space (e.g., Re-α space), predictions for flows with parameters in the neighborhood of the decomposition values can be calculated quickly by the ordinary differential equation system. The method could then be used as a design tool for control of the flow, e.g., to prevent or delay separation and transition.

Acknowledgments

This work was performed while the authors were in residence at the Program in Applied and Computational Mathematics, Princeton University. Support from the program is gratefully acknowledged. We also wish to thank Mark Stewart for assistance in producing a suitable grid.

References

[1]Patera, A. T., "A Spectral Element Method for Fluid Dynamics; Laminar Flow in a Channel Expansion," *Journal of Computational Physics,* Vol. 54, No. 3, 1984, pp. 468–488.

[2]Karniadakis, G. E., "Spectral Element Simulations of Laminar and Turbulent Flows in Complex Geometries," *Applied Numerical Mathematics,* Vol. 6, Dec. 1989/90, pp. 85–105.

[3]Lumley, J. L., *Stochastic Tools in Turbulence,* Academic Press, New York, 1970.

[4]Sirovich, L., "Turbulence and the Dynamics of Coherent Structures, Parts I, II and III," *Quarterly of Applied Mathematics,* Vol. XLV, No. 3, 1987, pp. 561–590.

[5]Deane, A. E., Kevrekidis, I. G., Karniadakis, G. E., and Orszag, S. A., "Low-Dimensional Models for Complex Geometry Flows: Application to Grooved Channels and Circular Cylinders," *Physics of Fluids A,* Vol. 3, No. 10, October 1991, pp. 2337–2354.

[6]Gharib, M., and Williams-Stuber, K., "Experiments on the Forced Wake of an Airfoil," *Journal of Fluid Mechanics,* Vol. 208, Nov. 1989, pp. 225–255.

[7]Williams-Stuber, K., and Gharib, M., "Transition from Order to Chaos in the Wake of an Airfoil," *Journal of Fluid Mechanics,* Vol. 213, April 1990, pp. 29–57.

[8]Sreenivasan, K. R., "Transition and Turbulence in Fluid Flows and Low Dimensional Chaos," *Frontiers in Fluid Mechanics,* edited by S. H. Davis and J. L. Lumley, Springer-Verlag, Berlin, 1985, pp. 41–67.

[9]Maday, Y., and Patera, A. T., "Spectral Element Methods for the Navier-Stokes Equations," *State-of-the-Art Surveys in Computational Mechanics,* edited by A. K. Noor, American Society of Mechanical Engineers, New York, 1988, pp. 71–143.

[10]Krause, E., Ehrhardt, G., and Schweitzer, B., "Experiments on Unsteady Flows about Wing Sections," *Proceedings of 2nd International Symposium on the Technology and Science of Low Speed and Motorless Flight,* Massachusetts Inst. of Technology, Cambridge, MA, 1974.

[11]Stewart, M. E. M., "General Decomposition Algorithm Applied to Multi-Element Airfoil Grids," AIAA Paper 90-1606, June 1990.

[12]Mavriplis, C., "A Posteriori Error Estimators for Adaptive Spectral Element Techniques," *Proceedings of the Eighth GAMM Conference on Numerical Methods in Fluid Mechanics,* Vol. 29, Vieweg, Braunschweig, Germany, 1990, pp. 333–342.

[13]Karniadakis, G. E., Israeli, M., and Orszag, S. A., "High-Order Splitting Methods for the Incompressible Navier-Stokes Equations," *Journal of Computational Physics,* Vol. 97, Dec. 1991, pp. 414–443.